PAPER

Green-synthesised cerium oxide nanostructures (CeO$_2$-NS) show excellent biocompatibility for phyto-cultures as compared to silver nanostructures (Ag-NS)

Qaisar Maqbool [ID] *[ab]

The use of nanostructures (NS) in plant tissue culture can be beneficial only if we have their complete bio-safety and biocompatibility profile. In the recent past, increasing rate of NS-cytotoxicity has alarmed the plant biotechnologist to think critically. Keeping this in view, our current study represents a comparative cytotoxicity examination of green fabricated highly potent CeO$_2$-NS and Ag-NS. Phyto-reductants from *O. europaea* extract simultaneously acted as reducing as well as capping agent in tuning the shape of CeO$_2$-NS and Ag-NS to as small as 18 nm and 26 nm respectively. High-performance liquid chromatography (HPLC) analysis of *O. europaea* extract supplemented by thermo-gravimetric analysis (TGA) findings further validates the capping action of bioactive agents from the plant extract. X-ray diffraction (XRD) testing confirms the phase purity and crystalline nature of prepared CeO$_2$-NS and Ag-NS. Fourier transform infrared (FTIR) spectroscopy shows typical Ce−O bond vibrations at 457 cm^{-1} and Ag around 563 cm^{-1} to 641 cm^{-1}. Moreover, the optimized NS shows differential cytotoxicity when tested on callogenesis and organogenesis of *Lycopersicon esculentum*. Findings from DPPH assay shows that CeO$_2$-NS are biocompatible and have tremendously enhanced the antioxidant potential of *L. esculentum* with greater biomass, contrastingly Ag-NS are found phyto-toxic with lower antioxidant potential and have a negative impact when added during plant tissue culture.

Introduction

Recent advancements in nanoscience and nanotechnology give birth to an interdisciplinary emerging field of nano-biotechnology. Nowadays, various types of metallic oxide NS have been engineered and due to their unique features like extremely small size, tuned bandgap energies with room temperature activation, higher surface to charge ratio, greater absorbability, low dosage and higher catalytic efficiency, they have shown promising results when tested on a variety of plant tissues.[1–3] Plant tissue culture techniques have been immensely supplemented with the blessings of latest optimized NS. Interesting findings have been reported so far showing enhancement in callus induction and organogenesis when metallic oxide NS were applied in low dosage. Some of the metallic oxide NS like Zn, Ce, Ag and Cu have shown overall improvement in plant growth dynamics when tested at optimum concentrations.[4] However, some studies also reported cytotoxicity of Ag and Ce based NS to plant tissues primarily due to ROS generation and heavy metal ion cytotoxicity and genotoxicity.[5,6]

Active cellular plant metabolism in the presence of O$_2$ generates ROS in variable amounts. These ROS, mainly free hydroxyl or oxygen radical species will quickly target the cell vital components like mitochondria, cell cycle signalling proteins, chromatin material, and even damage the cell envelope too. Cell self ROS-defense mechanism will try to cope with these lethal ROS by activating ROS scavenging and tolerating enzymes like peroxidases, catalases and superoxide dismutase.[7] It is interestingly observed that sometimes applied metallic oxide NS show synergistic behaviour to overcome the ROS effects primarily due to variable oxidation states of NS which generates redox cycle to hack the ROS.[8,9] These enzymes mimic characteristics are well reported by Ce based NS. In contrast, Ag based NS show cytotoxicity. Aqueous based Ag-NS are found toxic when experimented on the physiology of radish (*R. sativus*) plant.[10] Previous investigation also reported that Ag-NS effect on onion (*A. cepa*) is concentration dependent,[11] while Souza *et al.* reported that Ag-NS cause mitotic breaks at cell cycle and interrupt the normal functionality of the cell.[12] So there is an interesting debate in the safe mode application of Ag and Ce metallic oxide NS at the cellular level.

Thanks to the unique physicochemical characteristics of CeO$_2$-NS due to which they possess broad range of biomedical and plant-biotechnological applications.[13] Antioxidant potential of CeO$_2$-NS has been detected during rice seedling with boosted growth rate.[14]

[a]National Institute of Vacuum Science and Technology (NINVAST), NCP Complex, Islamabad, Pakistan. E-mail: Qaisar.vu@gmail.com

[b]Department of Biotechnology, Virtual University of Pakistan, Lahore, Pakistan

It was also reported that lipid homeostasis and ionic balance in corn plant was not altered when CeO₂-NS were applied to soil environment.[15] However, in case of soybean plant, CeO₂-NS at relatively high concentration show nitrogen cycle disturbance and reduced plant growth.[16] Meanwhile, in case of tomato, CeO₂-NS tremendously supplemented the growth factors with a positive effect at concentration of less than 10 mg L⁻¹. Inconsistent behaviour of CeO₂-NS may be due to variable particle size, plant type, different culture media or the use of different CeO₂-NS synthesis techniques.[17]

L. esculentum have been placed in one of the vast cultivated economically important nutritive crop worldwide and only in Pakistan *L. esculentum* have been cultivated at 62 930 ha area with annual yield of 95 279 hg ha⁻¹ in 2014.[18] Lycopene, vitamin C and A are the important nutritive constituents in *L. esculentum* having reported antioxidant potential at cellular level. These bioactive compounds shield the cells from ROS induced apoptosis.[19,20] Because of all these important features, we have chosen this economically important plant for our current study.

Keeping in view the role of nano-biotechnology in improving the agronomic value of *L. esculentum*, our team have bio-synthesized Ag and CeO₂-NS in order to check the potential role of these two metallic oxide NS in *L. esculentum* tissue culture. Our main targeted area is to examine the differential nano-toxicity and to find more suitable candidates in favor of *L. esculentum* growth dynamics. We promisingly believe that our comparative findings will provide a fruitful contribution to the knowledge of plant tissue culture.

Experimental section

Bio-synthesis of Ag-NS and CeO₂-NS

O. europaea leaves were procured from NARC (National Agricultural Research Centre), Pakistan. Leaf extract was made using our previously reported method.[13] For biosynthesis of CeO₂-NS, 8.68 g salt of Ce(NO₃)₃·6H₂O (Sigma Aldrich) was allowed to react with 200 mL of prepared leaves extract. Hot plate magnetic stirrer has been used with reaction condition of 50 °C, 1500 rpm for 2 hours. In order to separate the prepared pellets, centrifugation were performed at 12 000 rpm. Brownish colour pellets were collected. Moreover, to eliminate the impurities, centrifuges CeO₂-NS pellets were washed three times with ddH₂O. In the next step, CeO₂-NS pellets were dried under hot air oven at 60 °C for 6 hours and further annealed in blast furnace at 500 °C for 2 hours.

For green synthesis of Ag-NS, 6.796 g salt of AgNO₃ (Sigma Aldrich) was allowed to react with 200 mL of prepared leaves extract. The remaining synthesis methodology is same as described above for CeO₂-NS, the only difference was the adjustment of hot air oven to 50 °C. For better understanding of this facile synthesis route, we have generated the schematic diagram of the whole process as shown in Fig. 1.

Vibrational and optical studies of Ag-NS and CeO₂-NS

To examine the molecular nature of as prepared Ag-NS and CeO₂-NS, FT-IR spectroscopic studies were performed with specified NICOLET-6700 FTIR spectrometer model. In order to
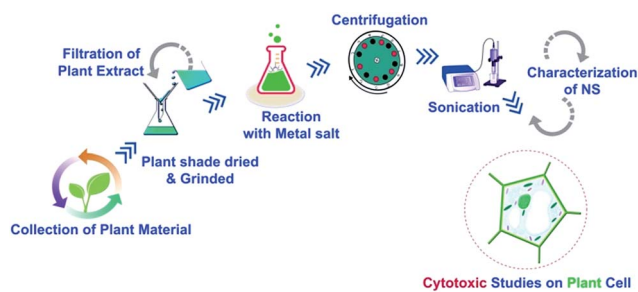

Fig. 1 Schematic diagram of fabrication of Ag-NS and CeO₂-NS using *O. europaea* leaf extract.

obtain KBr pellets of Ag-NS and CeO₂-NS, the hydraulic presser technique is followed. Moreover, FT-IR spectra showing stretching mode of vibrations in the structural phase of Ag-NS and CeO₂-NS were also recorded.

UV-visible absorption spectroscopy (Model "Perkin Elmer Lambda-200") was also conducted. In this process, the Ag-NS and CeO₂-NS powder sample were dissolved separately in ddH₂O and then UV-absorption spectra were recorded for further assessment.

Structural and morphological investigation of Ag-NS and CeO₂-NS

Crystallographic orientation of Ag and CeO₂-NS was carried using PANalytical-X'Pert³; Powder instrument. The instrument was setup at room temperature with operating voltage of 40 kV, diffraction angel (2θ) between 20° to 80° using Cu Kα radiation source having wavelength of 1.5406 Å. To calculate crystallite size of NS, Scherer's equation $[D = K\lambda/\beta \cos \theta]$ is employed, where D is the average crystalline domain size perpendicular to the reflecting planes, K is the Scherrer coefficient (0.85), λ is the X-ray wavelength (1.5406 Å), β is the angular full width at half maximum (FWHM) in radians, and θ is the diffraction angle (2 theta (degree) is the measured angle of diffraction in degrees) or Bragg's angle.

To examine as prepared Ag-NS and CeO₂-NS morphology, SEM analysis was performed *via* JOEL-JSM-6490LA-SEM operating at 20 kV together with Energy Dispersive X-ray (EDX) spectroscopy for elemental analysis.

HPLC and TGA analysis (for examination of capping bio-agent and capping action in Ag-NS/CeO₂-NS)

For comprehensive analysis of bio-active agents from *O. europaea* leaf extract, HPLC analysis was conducted following the scheme as reported in our previous studies[21] with minor adjustments. A mixture of 60% aqueous methanol (30 mL) with 5 g fine powder of *O. europaea* leaf added was prepared. The prepared mixture was put in centrifugation for 10 minutes at 2000 rpm. In next step, the centrifuged product was subject to ultra-filtration in 0.22 μm pore size micro-filter. After filtration, the mixture was installed in HPLC (Agilent Tech. Machine). CH₃CN solution (A) and 0.5% CH₃COOH solution (B) was taken as mobile phase. The operating temperature of HPLC column was set at 25 °C with flow speed of 1 mL per minute. Graph showing the sample examination were generated showing elution time (t_o) of unretained peak and retention time (t_R).

Capping action around as prepared Ag-NS and CeO$_2$-NS were further analyzed *via* TGA. This test is also important to evaluate the thermal stability of green fabricated Ag-NS and CeO$_2$-NS. The testing was conducted utilizing PerkinElmer Diamond_-TGA within nitrogen atmosphere. The temperature change was adjusted to 25 °C to 800 °C at 10 °C m^{-1}.

Collection and processing of plant material (*L. esculentum*)

L. esculentum seeds were procured from NARC. The explant was dehusked and immediately sterilized using 70% ethanol solution. N6 as basal media (having 3% sucrose sugar and 8 g L^{-1} GELRITE agar mixed) was used. After autoclaving the N6 medium, pH of the medium was adjusted to 5.8. Ag-NS and CeO$_2$-NS were added as supplementary material separately at different mg L^{-1} concentrations.

Callogenesis

To investigate callus induction, N6 media supplemented with Ag-NS in one group and CeO$_2$-NS in other was used. Medium (N6) without Ag-NS or CeO$_2$-NS were used as control. After this, the prepared cultured media (both of Ag-NS or CeO$_2$-NS) were exposed to 16/8 h day/night photoperiod for 14 days (at 25 ± 3 °C). Later on, callogenesis frequency was calculated using the following equation,

$$\text{Callogenesis frequency (\%)} = \frac{\text{no. of calli produced by explants}}{\text{no. of explants inoculated}} \times 100 \qquad (i)$$

Organogenesis (callus regeneration)

To examine organogenesis, embryonic-calli were transferred to different regeneration medium (MS + 1.0 Kin) supplemented with different mg L^{-1} concentrations of Ag-NS in one group and CeO$_2$-NS in other. Regeneration media without Ag-NS and CeO$_2$-NS were used as control. After the passage of 10 weeks, regeneration frequency were calculated *via* following relation,

$$\text{Organogenesis frequency (\%)} = \frac{\text{no. of explants regenerated into plantlets}}{\text{no. of explants inoculated for regeneration}} \times 100 \qquad (ii)$$

ROS scavenging activity

The ROS scavenging potential of Ag-NS and CeO$_2$-NS treated *L. esculentum* plants were examined through 2,2-diphenyl-1-picryl hydrazyl (DPPH). 90 μL of DPPH reagent was allowed to mixed with 10 μL of plant extract and incubated in dark for 60 minutes. Later on, the optical density of the mixture was estimated at 515 nm with a microplate reader. DMSO was used as negative control agent while ascorbic acid was treated as a positive control. The percentage scavenging activity of the sample was calculated using following relation.

$$\% \text{ inhibition activity of the sample} = \% \text{ ROS scavenging activity} = (1 - Ab_s/Ab_c) \times 100$$

In above relation, Ab_s is the absorbance of DPPH reagent mixed with sample, and Ab_c designates the absorbance of DMSO (negative control).

Results and discussion

Bio-synthesis process of Ag-NS and CeO$_2$-NS (study of capping action around NS)

O. europaea leaves extract mediated synthesis of Ag-NS and CeO$_2$-NS have great advantages over other conventional biofabrication techniques using bacteria or fungi. This is mainly because of greater biocompatibility, low cost and environmental friendly behaviour of plant extract. Bacteria or fungi based biosynthesis also requires optimized culture management and issues like contamination problems, NS isolation, microbial cellular mutations and bulk production for industrial usage.[13,22,23]

O. europaea leaves extract was evaluated through HPLC to find the potential bioactive molecules acting as reducing and capping agent around Ag-NS and CeO$_2$-NS. HPLC examination of the extract is shown in Fig. 2. Different peaks correspond to a variety of isolated bio-molecules traced through their specific retention time (t_R). The traced biomolecules from extract were reutin ($t_R = 6.6$), oleuropeosides (also called verbascoside) ($t_R = 7.8$), luteolin-7-*O*-glucoside (flavones) ($t_R = 8.6$), apigenin-7-*O*-glucoside ($t_R = 16.3$) oleuropein ($t_R = 23.5$) and oleuroside ($t_R = 33.9$). Findings clearly indicate that oleuropein and oleuroside are present in higher concentration. Among these two, oleuropein owns tremendous reducing power with higher ionizability in dissolution form. So it can be predicted that during capping action, it plays key role. It rapidly breaks down into elenolic acid and hydroxytyrosol.[13,21] Hydroxytyrosol due to higher polarizability behaviour than elenolic acid may take part as organic capping agent around Ag-NS and CeO$_2$-NS as hypothesized in Fig. 3.

It is important to further validate the capping agent and thermal properties of green synthesized Ag-NS and CeO$_2$-NS. In this connection comparative TGA analysis of Ag-NS and CeO$_2$-NS was made as shown in Fig. 4. TGA examination depicts
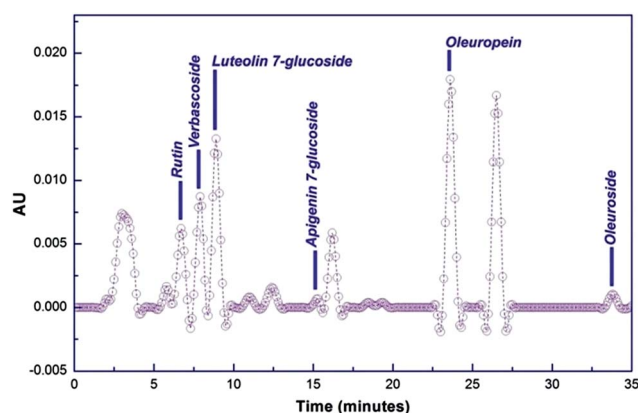

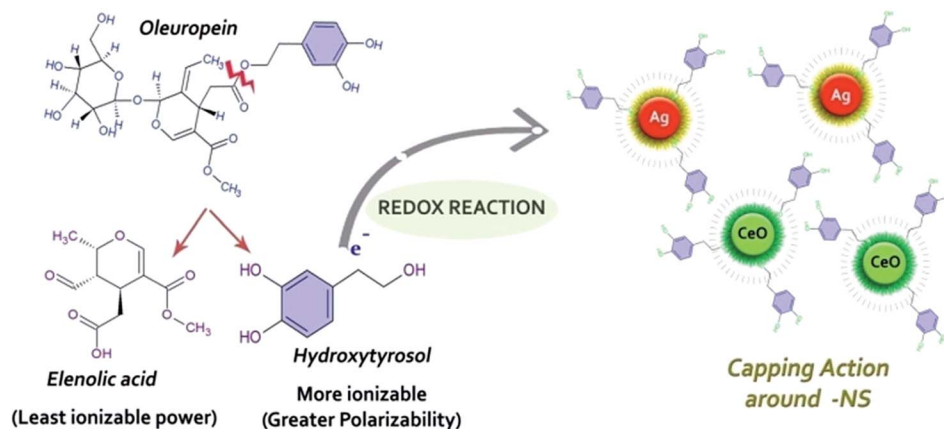**Fig. 2** Examination of bioactive compounds through HPLC analysis of leaves extract.

Fig. 3 Study of capping action around Ag-NS and CeO_2-NS.

different steps of Ag-NS and CeO_2-NS decompositions. In first two steps, both Ag-NS and CeO_2-NS samples show almost similar mass loss, the mass loss around 100 °C was due to surface adsorbed H_2O molecules. The mass loss around 80 to 200 °C was due to decomposition of bioactive organic molecules $(CHO)^{21,24}$ attached to the surface as active capping agents and this is also an evidence supporting involvement of bioactive compounds from *O. europaea* leaves extract. Moreover, the final step from TGA analysis shows differential decomposition behaviour as CeO_2-NS (sample) reflects prominent high temperature O_2 loss. High temperature O_2 loss by metallic oxide NS was also well supported from previous studies.[13,24] This

distortion in cure was not shown in Ag-NS (sample). Experimental findings show total mass loss of 0.53 mg (8.89%) by CeO_2-NS (sample) and 0.50 mg (8.81%) by Ag-NS (sample).

Vibrational and optical studies of Ag-NS and CeO_2-NS

Molecular characteristics with specific chemical bonding in as prepared CeO_2-NS and Ag-NS were examined using FT-IR spectroscopic studies, as shown in Fig. 5. The vibrational bond frequencies between 2200 cm^{-1} to 4000 cm^{-1} reflects surface adsorbed H–O–H, C–C, H–H, and C–H bond stretching prints.[13,25] The typical Ce–O stretch was traced at 457 cm^{-1}, well indexed to previously reported studies.[13] Moreover, vibrational frequencies at 563 cm^{-1}, 615 cm^{-1} and 641 cm^{-1} corresponds to Ag-NS.[25,26] No other stretching or vibrational modes were traced showing phase purity of as prepared CeO_2-NS and Ag-NS.

Optical parameters of green synthesized NS are of tremendous importance for achieving desired biomedical applications. Room temperature activation, surface activation energies, bandgap energies and visible light activation empowers the activities of NS inside the cellular environment.[27,28] Fig. 6 showing absorption peak of green synthesized CeO_2-NS at 298 nm and Ag-NS at 421 nm. Primarily these typical absorption peaks were originated due to the energy absorption which results in the electronic transitions between outer most energy shells. These typical UV absorption peaks were also seen in previously reported studies[13,26] and their appearance also validates the sample (CeO_2-NS and Ag-NS) purity.

Structural and morphological investigation of Ag-NS and CeO_2-NS

Crystallographic parameters of green synthesized CeO_2-NS and Ag-NS are shown in Fig. 7. All of the Bragg peaks marked in XRD spectrum of CeO_2-NS are well indexed to JCPDS card no. 340394 reflecting face centred cubic fluorite morphology of CeO_2-NS. Similarly Bragg peaks at (111), (200), (220) and (311) corresponds to Ag-NS experimental data (XRD) findings matched with JCPDS card no. 040783 showing face centred cubic structure of metallic Ag-NS. Moreover, appearance of XRD peaks at 27.79°, 32.17°, 46.15°, 54.54° & 57.55° showing the
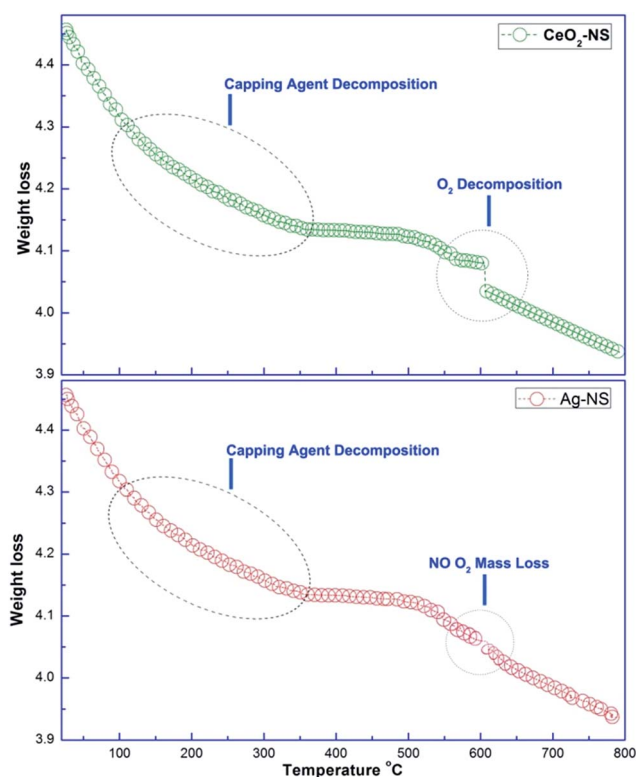

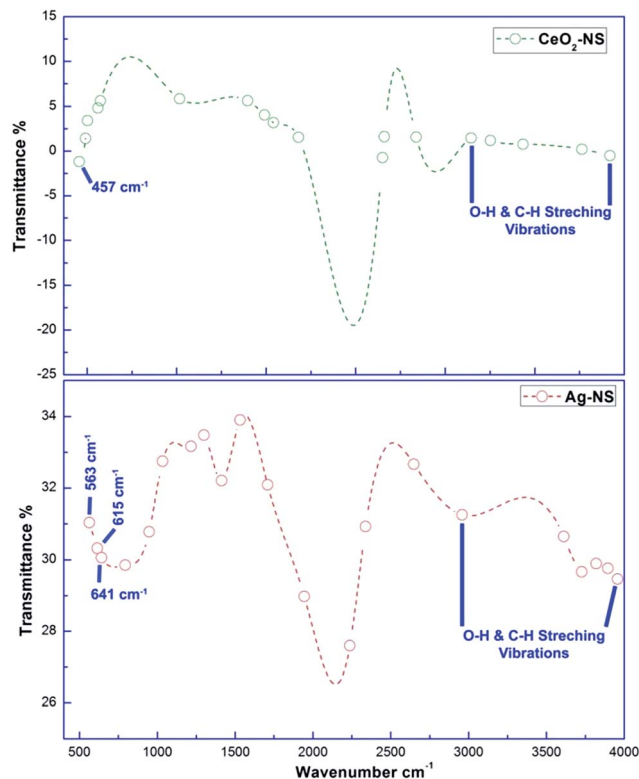**Fig. 4** Comparative TGA analysis of CeO_2-NS and Ag-NS.
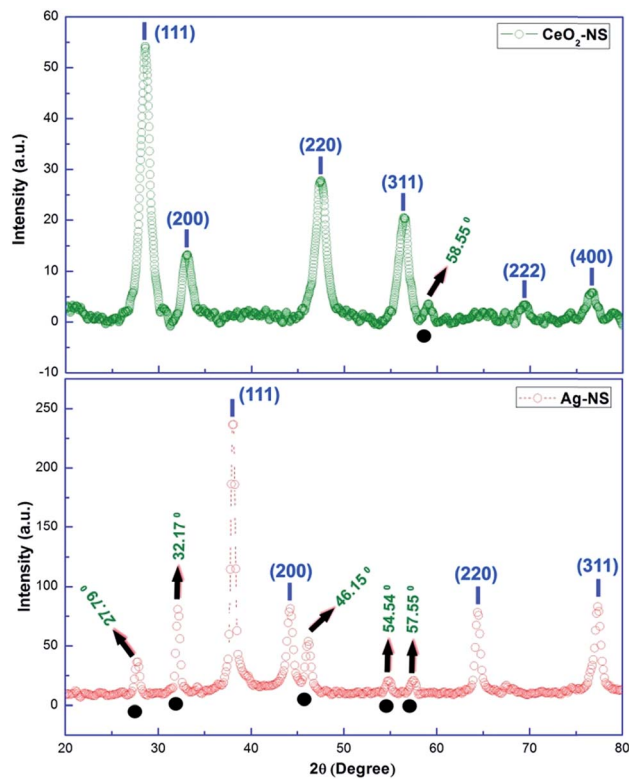
Fig. 5 FTIR spectrum of CeO₂-NS and Ag-NS.

Fig. 6 UV absorption spectrum of biosynthesized CeO₂-NS and Ag-NS.

Fig. 7 XRD peaks of CeO₂-NS and Ag-NS (note: peaks above black circles indicates crystallization of crystalline organometallic phase).
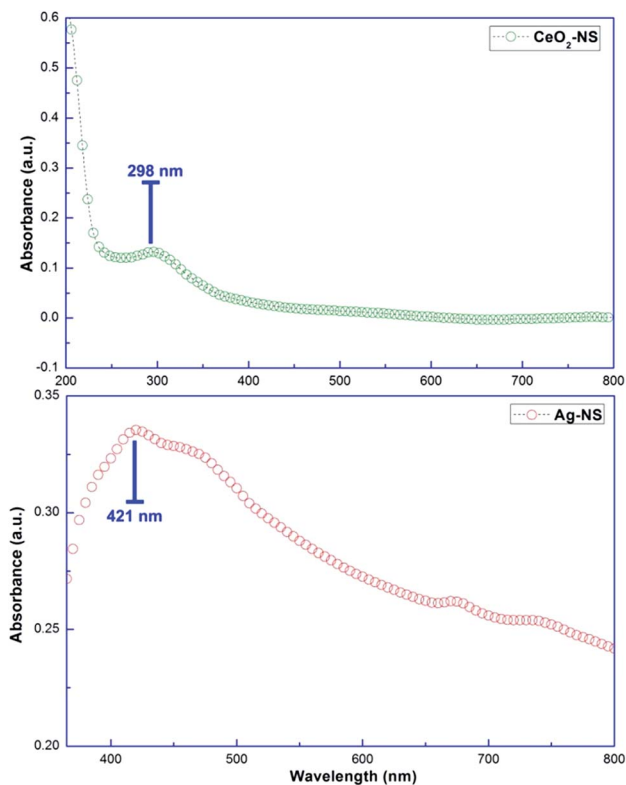
crystallization of crystalline organometallic phase. The appearance of similar XRD peaks have been observed before in Ag-NS synthesized from plant extract. However, these additional peaks can be resolved and ascribed to FCC structure of silver chloride (JCPDS no. 31-1238). This presence of chloride ions may probably attached from the leave extract of the plant during Ag-NS fabrication. Both of the synthesized samples show 100% phase purity without the presence of any impurity related to other metallic crystals. Keeping in view the prominent broad Bragg peak and from the calculations of Scherer equation, crystallite size of CeO₂-NS was found to be 7 nm. Moreover, the complexity of CeO₂-NS XRD spectrum is probably due to presence of crystalline organic metallic complex like at 58.55°. On the other hand, crystallite size of Ag-NS was found 10 nm. This smaller crystallite morphology plays important role in biological applications of NS.[29]

Smaller NS means greater surface area with maximum reactivity. SEM micrograph (Fig. 8) shows average CeO₂-NS size of 18.71 nm and Ag-NS size of 26.89 nm respectively. Both of the NS show uniform size and shape in SEM powder and dissolution form. EDX analysis of both the NS depicts pure chemical nature of the samples. Comparatively, CeO₂-NS are smaller than Ag-NS, these findings reflects that capping agent from leave extract tuned metallic oxide-NS size smaller than metallic-NS. This is probably due to the difference between high energy planes (atomic growth), difference in crystallite size, affinity and reactivity of capping agent, atomic size, electronic configuration and geometry of bounded O atoms in Ce crystal.[30,32] CeO₂-NS
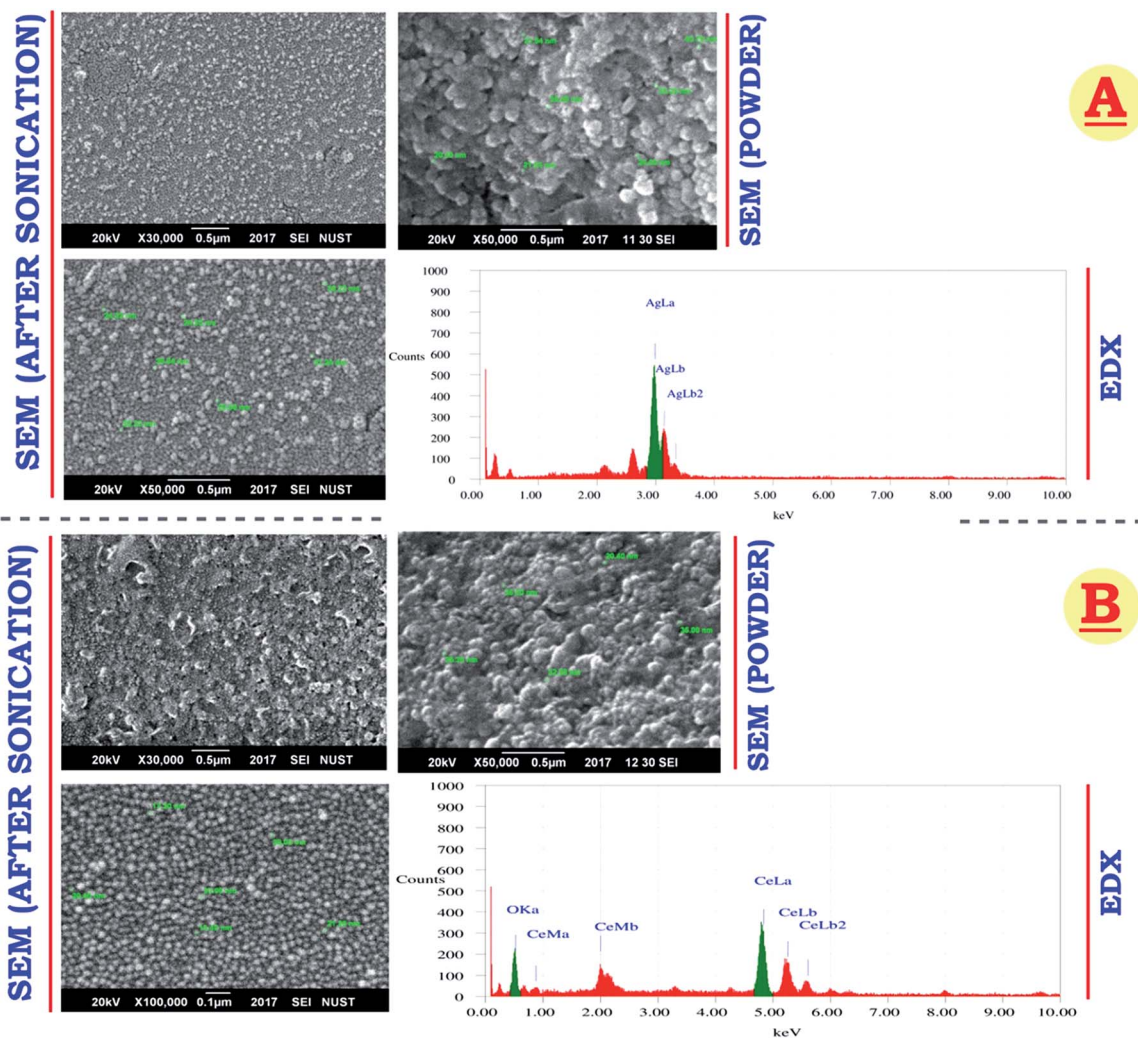
Fig. 8 SEM and EDX findings of Ag-NS (A) and CeO_2-NS (B).

having size less than 20 nm with potential biological activities are well reported before.[31]

Effect of CeO_2-NS and Ag-NS on callogenesis (callus induction) and organogenesis (direct shoot regeneration) of *L. esculentum*

Callus induction frequency of CeO_2-NS supplemented N6 media and Ag-NS supplemented N6 media on *L. esculentum* nodal and leaves explants are detailed in Table 1. Clearly, CeO_2-NS shows best performance at 6 mg mL^{-1} with 91% callogenesis in tissue taken from nodes and 88% in tissue taken from leaves explants as compared to the control group which is only 39% and 17% respectively. With similar concentration of 6 mg mL^{-1}, Ag-NS have not contributed any significant role in promoting callus induction. However, Ag-NS at the concentration of less than 3 mg mL^{-1} have shown no negative effect on callogenesis, but with the increase in concentration from 6 mg mL^{-1} to 10 mg mL^{-1}, progressive decline was observed. Ag-NS at the concentration of 10 mg mL^{-1} are found more toxic to the nodal explants tissue during callogenesis showing only 10% callus induction frequency. It was also keenly observed that at higher

dosage of CeO_2-NS (10 mg mL^{-1}), slight reduction in callogenesis as compared to low concentration (3 mg mL^{-1} and 6 mg mL^{-1}) was observed.

Likewise callus induction frequencies, CeO_2-NS have shown supplementary behaviour in organogenesis of both nodal and leave explants with the concentration of 3 mg mL^{-1} to 10 mg mL^{-1} in growth medium (MS + 0.1 mg L^{-1} Kin), as shown in Table 2. On the other hand, Ag-NS have reflected differential behavior for nodal explants and leave explants in organogenesis frequency. Ag-NS supplemented in growth medium have stunt the plant growth in leave explant showing no organogenesis. In nodal explants, upto the concentration of 6 mg mL^{-1}, organogenesis frequency of less then 15% was observed as compared to control group which is of 36%. It predicts phytotoxic behaviour of Ag-NS in both callus induction and organogenesis in comparison to CeO_2-NS supplementary behaviour.

The contrasting behaviour of metallic oxide-NS on plant tissues is primarily linked with difference in their NS chemical composition, particle size and morphology, specific crystallite size, NS-surface activation, cellular interaction, photo-activation and tuned bandgap energies.[3,4,33] Smaller NS size will ensure

Table 1 The callogenesis frequency at different concentration of CeO_2-NS (set-I) and Ag-NS (set-II)[a]

Explants (set-I)	N6-media + CeO_2-NS (mg L^{-1})			
	Control group	CeO_2-NS (3 mg L^{-1})	CeO_2-NS (6 mg L^{-1})	CeO_2-NS (10 mg L^{-1})
Nodes	11.20 ± 1.5b (39%)	15.33 ± 1.0b (51%)	28.17 ± 2.6a (91%)	13.00 ± 1.9c (30%)
Leaves	6.00 ± 0.2c (17%)	13.00 ± 0.0b (43%)	24.60 ± 2.3a (88%)	15.00 ± 0.01c (27%)

[a] LSD for media = 5.5930. LSD for explant = 4.5667. $p < 0.05$ (data followed by small alphabets stand for the individual values as an average of three replicates. Each replicate consisted of 10 treatments).

Explants (set-II)	N6-Media + Ag-NS (mg L^{-1})			
	Control group	Ag-NS (3 mg L^{-1})	Ag-NS (6 mg L^{-1})	Ag-NS (10 mg L^{-1})
Nodes	11.20 ± 1.5b (39%)	14.07 ± 1.6b (38%)	10.11 ± 1.6c (19%)	7.00 ± 1.3c (10%)
Leaves	6.00 ± 0.2c (16%)	10.00 ± 1.0c (30%)	7.14 ± 1.2c (16%)	8.00 ± 0.1c (14%)

Table 2 The organogenesis frequency at different concentration of CeO_2-NS (set-I) and Ag-NS (set-II)[a]

Explants (set-I)	Regeneration media + CeO_2-NS (mg L^{-1})			
	Control group	CeO_2-NS (3 mg L^{-1})	CeO_2-NS (6 mg L^{-1})	CeO_2-NS (10 mg L^{-1})
Nodes	10.33 ± 0.0c (36%)	14.00 ± 1.2b (51%)	19.13 ± 1.0b (65%)	20.16 ± 1.3a (81%)
Leaves	7.50 ± 1.2c (25%)	10.00 ± 1.0b (41%)	15.00 ± 0.0c (38%)	18.30 ± 1.1b (65%)

[a] LSD for explant = 4.142. $p < 0.05$ (data followed by small alphabets stand for the individual values as an average of three replicates. Each replicate consisted of 10 treatments).

Explants (set-II)	Regeneration media + Ag-NS (mg L^{-1})			
	Control group	Ag-NS (3 mg L^{-1})	Ag-NS (6 mg L^{-1})	Ag-NS (10 mg L^{-1})
Nodes	10.33 ± 0.0c (36%)	6.00 ± 1.3c (13%)	9.33 ± 1.1c (10%)	0.00 ± 0.0d (0%)
Leaves	7.50 ± 1.2c (25%)	0.00 ± 0.0d (0%)	00.00 ± 0.0d (0%)	0.00 ± 0.0d (0%)

maximum penetration to the cellular and sub-cellular structures. Normally, metallic oxide NS are surface positively charged which helps them in binding to the various cellular structures for chemical interaction.[4,13] Smaller size will also provide greater surface area to charge ratio. This will boost the rate of NS activation inside the cellular environment. Metallic oxide-NS also interact and enhance enzyme activity by promoting the metallic ions as activated co-factors for enzyme–substrate bridging.[34] Some of the recent investigations have shown that CeO_2-NS have promoted the functionality of enzymes involved in the catalysis of carbohydrate metabolism, bioactivity of phospholipids, terpenoids synthesis and metabolites tunning. Enhancement in enzyme performance will ultimately improve the biosynthetic machinery of the cell and this will encourage the cell growth and division.[34–36] CeO_2-NS possess selective molecular interaction, as in case of cucumber even at higher concentration of 800 mg kg^{-1}, Ce ions do not show any negative influence of chlorophyll performance or even any other photosynthetic pigments.[37] In previous studies, Ce at nanoscale have successfully promoted the overall growth dynamics of radish, wheat and economically important corn plant.[38–40] CeO_2-NS upto the concentration of 10 mg L^{-1} have shown long term positive effect on *L. esculentum* organogenesis.[17] But in our case,

green synthesized CeO_2-NS are found even more effective in increasing the callogenesis and organogenesis of *L. esculentum* at extremely small dosage of 6 mg mL^{-1}. This is probably due to the effect of biocompatible capping agent around NS. Green chemistry has augmented the biocompatibility of CeO_2-NS at cellular level and increase the overall biomass of *L. esculentum*. In contrast, low performance of Ag-NS may be due to alteration in cell homeostasis of macro and micro nutrients. It is well reported in past that Ag-NS can alter the absorption of Mg, Mn and Zn.[41] All these elements are involved in optimum activity of enzymes.[42] So, Ag-NS concentration in plant tissue can cause enzyme malfunctioning and growth arrest. Similar toxic effects of Ag-NS on plant tissue are also well reported previously.[10]

Studies in past have concluded that Ag-NS exhibits unpredictable behaviour when tested on plant tissues. Cytotoxic and genotoxic performance of Ag-NS are due to sedimentation and hyper-reactivity of these heavy Ag-NS causing metallic-ion induced toxicity to the cell. In case of *Arabidopsis* root, massive aggregation of extremely small size Ag-NS were observed causing cellular toxicity.[43] Presence of surface coating agents also produces different results towards the cytotoxic nature of Ag-NS. Probably, green synthesized Ag-NS exhibit more solubility because of bio-augmented capping agent.[44] This
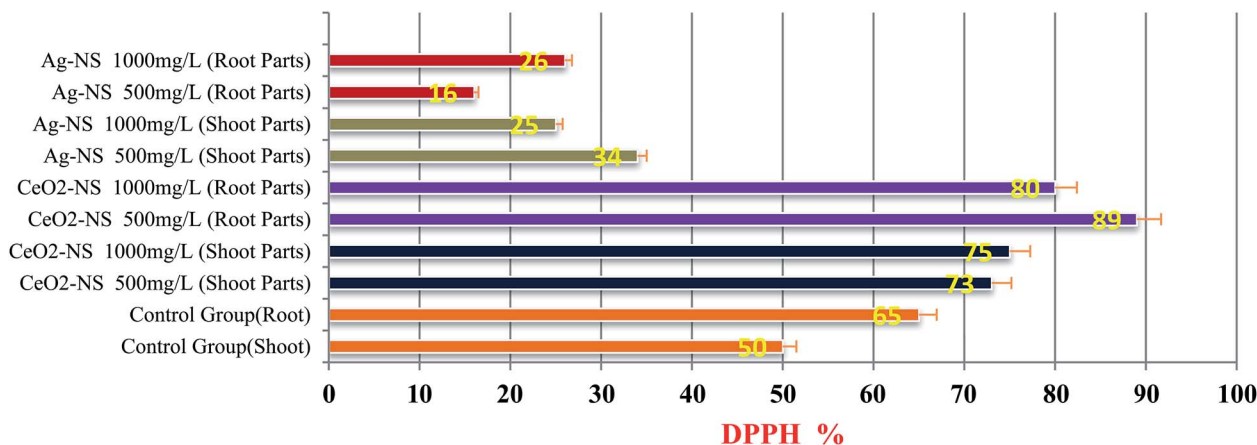
Fig. 9 Comparative analysis of ROS scavenging potential of NS treated plant tissues.

will cause Ag-NS to become more reactive when in contact with cellular and sub-cellular structures causing growth arrest. Due to all of these factors our experimental results show that *L. esculentum* tissue fails to tolerate Ag-NS during organogenesis.

ROS scavenging activity

ROS scavenging findings in Fig. 9 reflects differential behaviour of green fabricated CeO_2-NS and Ag-NS. CeO_2-NS have shown auspicious scavenging activity of up to 89% both in the case of tested shoot and root part extract. Interestingly, Ag-NS have not shown any promising results, only 26% scavenging activity was recorded in case of root extract.

This differential behaviour of CeO_2-NS and Ag-NS can be explained on the basis of difference in physicochemical parameters of both the materials. ROS scavenging activity mainly depends upon variable oxidation states[9] and redox potential of the material. Ce in comparison to Ag possess two different oxidation states of Ce^{3+} (Ce_2O_3) and Ce^{4+} (CeO_2), and can tolerate free radicals.[13,28,45] Normally it has been observed that Ce is present in CeO_2 form at CeO_2-NS surface having

deficient oxygen (O) and valency of Ce^{3+} rather than Ce^{4+}. This defect chemistry in the surface of pre-activated CeO_2-NS can provide maximum antioxidant potential to them.[45] Moreover, in CeO_2-NS, the interconversion of Ce^{3+} into Ce^{4+} in dissolution state can also provide smooth environment for antioxidant enzyme mimicry action. This can generate as well as can tolerate ROS cycle.[46,47] Here in our experimental observations, CeO_2-NS supplementation to growth medium of *L. esculentum* plant, have tremendously improved the antioxidant capacity at cellular and sub-cellular level which results in enhanced callogenesis and organogenesis. CeO_2-NS have successfully tolerated the variety of ROS as explained in Fig. 10. The multiple ROS degradation by CeO_2-NS (*via* redox cycle) during cellular metabolism can be described as follows,
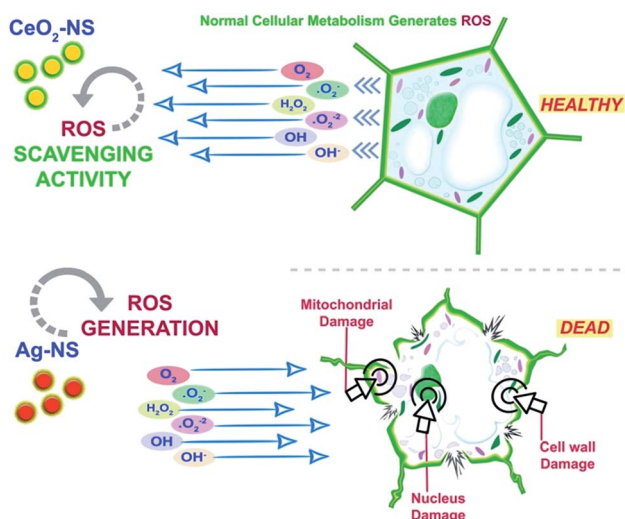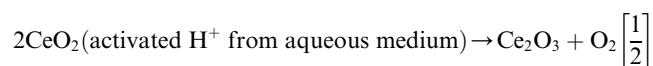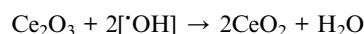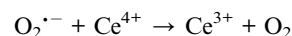
$$O_2^{\cdot-} + 2H^+ + Ce^{3+} \rightarrow Ce^{4+} + H_2O_2$$

$$H_2O_2 + 2Ce^{4+} + 2OH^- \rightarrow 2H_2O + O_2 + 2Ce^{3+}$$

$$O_2^{\cdot-} + Ce^{4+} \rightarrow Ce^{3+} + O_2$$

$$Ce_2O_3 + 2[\cdot OH] \rightarrow 2CeO_2 + H_2O$$

$$2CeO_2(\text{activated } H^+ \text{ from aqueous medium}) \rightarrow Ce_2O_3 + O_2\left[\frac{1}{2}\right]$$

$$Ce^{4+} + {}^{\cdot}NO \text{ (nitric oxide free radical)} \rightarrow Ce^{3+} + NO^+ \text{ (least toxic)}$$

On the other hand, Ag-NS have inhibited the organogenesis when supplemented in growth medium. This phytotoxic nature of Ag-NS may probably link with ROS in-toleration and heavy metal (Ag) induced necrosis.[48] ROS like ${}^{\cdot}O_2^-$ and H_2O_2 can cause direct DNA damage, mitochondrial malfunction and cell wall degeneration which results in loss of cell activity[49] and stunt cellular differentiation during callus induction or organogenesis. In our observations, both in the case of nodal and leaves explants, Ag-NS exposure causes phytotoxicity during callus induction and organogenesis of *L. esculentum*.

Fig. 10 Differential phytotoxicity of CeO_2-NS and Ag-NS.

Conclusion

This study concludes following outcomes:

• Green chemistry proves to be an efficient, cost-effective and environmental friendly method for the synthesis of highly optimized CeO_2-NS and Ag-NS. Phytochemicals from *O. europaea* extract have successfully tailored the NS acting as strong reducing and capping agents.

• HPLC and TGA findings validate the effective utilization of bio-capping agents from plant extract around both CeO_2-NS and Ag-NS.

• SEM and XRD reports show homogenous NS size with pure crystalline behaviour. FTIR also shows pure chemical nature of green synthesized NS.

• Green prepared NS show differential phytotoxicity towards *L. esculentum* callogenesis and organogenesis. Ag-NS are found nanotoxic to plant tissue due to the ROS induced necrosis while CeO_2-NS have shown tremendous ROS scavenging supplementary actions.

So, CeO_2-NS in future probably consider as strong candidate for the improvement of fertilizers efficiency. CeO_2-NS can be used as biocompatible nano-fertilizer in combination with other vital nutrients required for *L. esculentum* plant growth. Moreover, it is strongly proposed that medicinally important recalcitrant plants can be regenerated *via* tissue culture technique using ROS-scavenging CeO_2-NS as supplementary growth medium.

Conflicts of interest

There are no conflicts to declare.

Acknowledgements

Notes and references

1 H. Singh, J. Du and T. H. Yi, Green and rapid synthesis of silver nanoparticles using *Borago officinalis* leaf extract: anticancer and antibacterial activities, *Artif. Cells, Nanomed., Biotechnol.*, 2017, **45**(7), 1310–1316.

2 A. Martin and A. Sarkar, Overview on biological implications of metal oxide nanoparticle exposure to human alveolar A549 cell line, *Nanotoxicology*, 2017, **11**(6), 713–724.

3 S. Anwaar, Q. Maqbool, N. Jabeen, M. Nazar, F. Abbas, B. Nawaz, T. Hussain and S. Z. Hussain, The Effect of Green Synthesized CuO Nanoparticles on Callogenesis and Regeneration of *Oryza sativa* L., *Frontiers in plant science*, 2016, 7, 1330.

4 D. H. Kim, J. Gopal and I. Sivanesan, Nanomaterials in plant tissue culture: the disclosed and undisclosed, *RSC Adv.*, 2017, **7**(58), 36492–36505.

5 D. K. Tripathi, A. Tripathi, S. S. Shweta, Y. Singh, K. Vishwakarma, G. Yadav, S. Sharma, V. K. Singh, R. K. Mishra, R. G. Upadhyay and N. K. Dubey, Uptake, accumulation and toxicity of silver nanoparticle in autotrophic plants, and heterotrophic microbes: A concentric review, *Front. Microbiol.*, 2017, **8**, 7.

6 M. I. Morales, C. M. Rico, J. A. Hernandez-Viezcas, J. E. Nunez, A. C. Barrios, A. Tafoya, J. P. Flores-Marges, J. R. Peralta-Videa and J. L. Gardea-Torresdey, Toxicity assessment of cerium oxide nanoparticles in cilantro (*Coriandrum sativum* L.) plants grown in organic soil, *J. Agric. Food Chem.*, 2013, **61**(26), 6224–6230.

7 K. Das and A. Roychoudhury, Reactive oxygen species (ROS) and response of antioxidants as ROS-scavengers during environmental stress in plants, *Frontiers in Environmental Science*, 2014, **2**, 53.

8 J. Yang, W. Cao and Y. Rui, Interactions between nanoparticles and plants: phytotoxicity and defense mechanisms, *J. Plant Interact.*, 2017, **12**(1), 158–169.

9 G. Marslin, C. J. Sheeba and G. Franklin, Nanoparticles Alter Secondary Metabolism in Plants *via* ROS Burst, *Frontiers in plant science*, 2017, **8**, 832.

10 N. Zuverza-Mena, R. Armendariz, J. R. Peralta-Videa and J. L. Gardea-Torresdey, Effects of silver nanoparticles on radish sprouts: root growth reduction and modifications in the nutritional value, *Frontiers in plant science*, 2016, **7**, 90.

11 M. Kumari, A. Mukherjee and N. Chandrasekaran, Genotoxicity of silver nanoparticles in Allium cepa, *Sci. Total Environ.*, 2009, **407**(19), 5243–5246.

12 T. A. Souza, L. P. Franchi, L. R. Rosa, M. A. da Veiga and C. S. Takahashi, Cytotoxicity and genotoxicity of silver nanoparticles of different sizes in CHO-K1 and CHO-XRS5 cell lines, *Mutat. Res., Genet. Toxicol. Environ. Mutagen.*, 2016, **795**, 70–83.

13 Q. Maqbool, M. Nazar, S. Naz, T. Hussain, N. Jabeen, R. Kausar, S. Anwaar, F. Abbas and T. Jan, Antimicrobial potential of green synthesized CeO_2 nanoparticles from *Olea europaea* leaf extract, *Int. J. Nanomed.*, 2016, **11**, 5015.

14 C. M. Rico, J. Hong, M. I. Morales, L. Zhao, A. C. Barrios, J. Y. Zhang, J. R. Peralta-Videa and J. L. Gardea-Torresdey, Effect of cerium oxide nanoparticles on rice: a study involving the antioxidant defense system and *in vivo* fluorescence imaging, *Environ. Sci. Technol.*, 2013, **47**(11), 5635–5642.

15 K. Birbaum, R. Brogioli, M. Schellenberg, E. Martinoia, W. J. Stark, D. Günther and L. K. Limbach, No evidence for cerium dioxide nanoparticle translocation in maize plants, *Environ. Sci. Technol.*, 2010, **44**(22), 8718–8723.

16 Z. Cao, C. Stowers, L. Rossi, W. Zhang, L. Lombardini and X. Ma, Physiological effects of cerium oxide nanoparticles on the photosynthesis and water use efficiency of soybean (*Glycine max* (L.) Merr.), *Environ. Sci.: Nano*, 2017, **4**(5), 1086–1094.

17 Q. Wang, X. Ma, W. Zhang, H. Pei and Y. Chen, The impact of cerium oxide nanoparticles on tomato (*Solanum lycopersicum* L.) and its implications for food safety, *Metallomics*, 2012, **4**(10), 1105–1112.

18 Food and Agriculture Organization of the United Nations, http://www.fao.org/faostat.

19 P. M. Choksi and V. Y. Joshi, A review on lycopene—extraction, purification, stability and applications, *Int. J. Food Prop.*, 2007, **10**(2), 289–298.

20 E. Elbadrawy and A. Sello, Evaluation of nutritional value and antioxidant activity of tomato peel extracts, *Arabian J. Chem.*, 2016, **9**, S1010–S1018.

21 Q. Maqbool, S. Iftikhar, M. Nazar, F. Abbas, A. Saleem, T. Hussain, R. Kausar, S. Anwaar and N. Jabeen, Green fabricated CuO nanobullets *via Olea europaea* leaf extract shows auspicious antimicrobial potential, *IET Nanobiotechnol.*, 2017, **11**(4), 463–468.

22 F. Charbgoo, M. B. Ahmad and M. Darroudi, Cerium oxide nanoparticles: green synthesis and biological applications, *Int. J. Nanomed.*, 2017, **12**, 1401.

23 I. Hussain, N. B. Singh, A. Singh, H. Singh and S. C. Singh, Green synthesis of nanoparticles and its potential application, *Biotechnol. Lett.*, 2016, **38**(4), 545–560.

24 R. Suresh, V. Ponnuswamy and R. Mariappan, Effect of annealing temperature on the microstructural, optical and electrical properties of CeO_2 nanoparticles by chemical precipitation method, *Appl. Surf. Sci.*, 2013, **273**, 457–464.

25 V. Manikandan, P. Velmurugan, J. H. Park, W. S. Chang, Y. J. Park, P. Jayanthi, M. Cho and B. T. Oh, Green synthesis of silver oxide nanoparticles and its antibacterial activity against dental pathogens, *3 Biotech*, 2017, **7**(1), 72.

26 R. Kausar, M. A. Shaheen, Q. Maqbool, S. Naz, M. Nazar, F. Abbas, T. Hussain, U. Younas and M. F. Shams, Facile biosynthesis of Ag-NPs using *Otostegia limbata* plant extract: Physical characterization and auspicious biological activities, *AIP Adv.*, 2016, **6**(9), 095203.

27 B. H. Kim, M. J. Hackett, J. Park and T. Hyeon, Synthesis, characterization, and application of ultrasmall nanoparticles, *Chem. Mater.*, 2013, **26**(1), 59–71.

28 F. Abbas, J. Iqbal, Q. Maqbool, T. Jan, M. O. Ullah, B. Nawaz, M. Nazar, M. H. Naqvi and I. Ahmad, ROS mediated malignancy cure performance of morphological, optical, and electrically tuned Sn doped CeO_2 nanostructures, *AIP Adv.*, 2017, **7**(9), 095205.

29 F. Abbas, Q. Maqbool, M. Nazar, N. Jabeen, S. Z. Hussain, S. Anwaar, N. Mehmood, M. S. Sheikh, T. Hussain and S. Iftikhar, Green synthesised zinc oxide nanostructures through *Periploca aphylla* extract shows tremendous antibacterial potential against multidrug resistant pathogens, *IET Nanobiotechnol.*, 2017, 935–941.

30 Z. Lu, K. Rong, J. Li, H. Yang and R. Chen, Size-dependent antibacterial activities of silver nanoparticles against oral anaerobic pathogenic bacteria, *J. Mater. Sci.: Mater. Med.*, 2013, **24**(6), 1465–1471.

31 Z. Niu and Y. Li, Removal and utilization of capping agents in nanocatalysis, *Chem. Mater.*, 2013, **26**(1), 72–83.

32 E. Alpaslan, B. M. Geilich, H. Yazici and T. J. Webster, pH-Controlled Cerium Oxide Nanoparticle Inhibition of Both Gram-Positive and Gram-Negative Bacteria Growth, *Sci. Rep.*, 2017, **7**, 45859.

33 B. Samai, S. Sarkar, S. Chall, S. Rakshit and S. C. Bhattacharya, Polymer-fabricated synthesis of cerium oxide nanoparticles and applications as a green catalyst towards multicomponent transformation with size-dependent activity studies, *CrystEngComm*, 2016, **18**(40), 7873–7882.

34 M. Chen, G. Zeng, P. Xu, C. Lai and L. Tang, How Do Enzymes 'Meet'Nanoparticles and Nanomaterials?, *Trends Biochem. Sci.*, 2017, 914–930.

35 L. Shang, K. Nienhaus and G. U. Nienhaus, Engineered nanoparticles interacting with cells: size matters, *J. Nanobiotechnol.*, 2014, **12**(1), 5.

36 Ž. Krpetić, S. Anguissola, D. Garry, P. M. Kelly and K. A. Dawson, Nanomaterials: impact on cells and cell organelles, in *Nanomaterial*, Springer Netherlands, 2014, pp. 135–156.

37 Y. Rui, P. Zhang, Y. Zhang, Y. Ma, X. He, X. Gui, Y. Li, J. Zhang, L. Zheng, S. Chu and Z. Guo, Transformation of ceria nanoparticles in cucumber plants is influenced by phosphate, *Environ. Pollut.*, 2015, **198**, 8–14.

38 X. Gui, M. Rui, Y. Song, Y. Ma, Y. Rui, P. Zhang, X. He, Y. Li, Z. Zhang and L. Liu, Phytotoxicity of CeO_2 nanoparticles on radish plant (*Raphanus sativus*), *Environ. Sci. Pollut. Res.*, 2017, 1–7.

39 C. M. Rico, J. R. Peralta-Videa and J. L. Gardea-Torresdey, Differential effects of cerium oxide nanoparticles on rice, wheat, and barley roots: A Fourier Transform Infrared (FT-IR) microspectroscopy study, *Appl. Spectrosc.*, 2015, **69**(2), 287–295.

40 Z. Yang, J. Chen, R. Dou, X. Gao, C. Mao and L. Wang, Assessment of the phytotoxicity of metal oxide nanoparticles on two crop plants, maize (*Zea mays* L.) and rice (*Oryza sativa* L.), *Int. J. Environ. Res. Public Health*, 2015, **12**(12), 15100.

41 M. K. Sarmast and H. Salehi, Silver nanoparticles: An influential element in plant nanobiotechnology, *Mol. Biotechnol.*, 2016, **58**(7), 441–449.

42 A. B. Morales-Díaz, H. Ortega-Ortíz, A. Juárez-Maldonado, G. Cadenas-Pliego, S. González-Morales and A. Benavides-Mendoza, Application of nanoelements in plant nutrition and its impact in ecosystems, *Adv. Nat. Sci.: Nanosci. Nanotechnol.*, 2017, **8**(1), 013001.

43 N. Y. Selivanov, O. G. Selivanova, O. I. Sokolov, M. K. Sokolova, A. O. Sokolov, V. A. Bogatyrev and L. A. Dykman, Effect of gold and silver nanoparticles on the growth of the Arabidopsis thaliana cell suspension culture, *Nanotechnol. Russ.*, 2017, **12**(1–2), 116–124.

44 A. Rónavári, D. Kovács, N. Igaz, C. Vágvölgyi, I. M. Boros, Z. Kónya, I. Pfeiffer and M. Kiricsi, Biological activity of green-synthesized silver nanoparticles depends on the applied natural extracts: a comprehensive study, *Int. J. Nanomed.*, 2017, **12**, 871.

45 J. S. Cresi, M. C. Spadaro, S. D'Addato, S. Valeri, L. Amidani, F. Boscherini, G. Bertoni, D. Deiana and P. Luches, Contraction, cation oxidation state and size effects in cerium oxide nanoparticles, *Nanotechnology*, 2017, 495702.

Paper

46 S. Singh, Cerium oxide based nanozymes: Redox phenomenon at biointerfaces, *Biointerphases*, 2016, **11**(4), 04B202.

47 S. Soren, S. R. Jena, L. Samanta and P. Parhi, Antioxidant potential and toxicity study of the cerium oxide nanoparticles synthesized by microwave-mediated synthesis, *Appl. Biochem. Biotechnol.*, 2015, **177**(1), 148–161.

48 S. B. Vasanth and G. A. Kurian, Toxicity evaluation of silver nanoparticles synthesized by chemical and green route in different experimental models, *Artif. Cells, Nanomed., Biotechnol.*, 2017, 1721–1727.

49 R. Wan, Y. Mo, L. Feng, S. Chien, D. J. Tollerud and Q. Zhang, DNA damage caused by metal nanoparticles: the involvement of oxidative stress and activation of ATM, *Chem. Res. Toxicol.*, 2012, **25**(7), 1402.